A macroscopic- and microscopic structural view on the deposition of the Ekströmsberg iron mineralization

David Jargvoll

Degree of Bachelor of Science
with a major in Earth Sciences
15 hec

Department of Earth Sciences
University of Gothenburg
2023 B-1235

Faculty of Science

UNIVERSITY OF GOTHENBURG

UNIVERSITY OF GOTHENBURG
Department of Earth Sciences
Geovetarcentrum/Earth Science Centre

A macroscopic- and microscopic structural view on the deposition of the Ekströmsberg iron mineralization

David Jargvoll

ISSN 1400-3821

B1235
Bachelor of Science thesis
Göteborg 2023

Mailing address
Geovetarcentrum
S 405 30 Göteborg

Address
Geovetarcentrum
Guldhedsgatan 5A

Telephone
031-786 19 56

Geovetarcentrum
Göteborg University
S-405 30 Göteborg
SWEDEN

Foreword

This bachelor thesis has been produced at the Department of Earth Sciences, University of Gothenburg under the supervision of Professor Robert Hellingwerf, and Mark Johnson

I would like to thank the guys at GIAB for making this possible and providing for a very memorable summer in the beautiful north of Sweden.

Special thanks go to Robert Hellingwerf for giving me this opportunity and for his guidance, support, and good mood up to the very end.

I am greatly appreciative for having met the colourful entourage of assistants; Carl *Bear-scare* Groenberg, Jimmy *¨I think I'll be mass murderer when I grow up¨* Ukkola and Filip *the rock* Sundquist.

But most of all I'd like to thank Joakim Nordstrand, a never-ending source of optimism and good suggestions. Like the first time we sat down in the outdoor tub. He said: Let's keep drinking and not get up before the sun sets. I'm sad to say that 5 weeks later in the beginning of August the sun finally set.

Table of Contents

The Ekströmsberg mineralization 7
History and location 7
Regional geological setting 7
Local geological setting 8
Suggested theories for genesis and deposition 8
Method 10
Field map 10
Drill holes 13
Malå drill core storage 14
Thin sections 14
Compiling of data and drill core projections 16
Data and map accuracy 19
Results and observations 20
Field observations 20
Thin section observations 26
Faults and fractures 28
Malå drill core storage observations 28
Discussion 29
Conclusions 31
Works cited 32
Appendix 1 – 5 34
Appendix 1: Area description 34
Appendix 2: field observations with coordinates and fractures 37
Appendix 3: Thin section description 40
Appendix 4: chemical test samples 44
Appendix 5: Location of images used in thesis 45

List of Figures

Figure 1 - Arial photo showing the town of Kiruna to the right and the surveyed area indicated by the arrow 7
Figure 2 - Tools used in the field. Notebook, hammer, GPS, magnet (sticking to the side of the outcrop) 10
Figure 3 - Strike, dip and lager faults 12
Figure 4 - Magnetite core at Malå drill core storage 14
Figure 5 - Thin section location 15
Figure 6 - Original drill hole protocol with offset and re-scaled interpretation on top. The yellow circles show plunge observed in area. 16
Figure 7 - Drill-hole projections 17
Figure 8 - Field observation map 18
Figure 9 - Magnetite typical of Ekströmsberg 20
Figure 10 - Hematite typical of Ekströmsberg 20
Figure 11 - Final Map of Ekströmsberg mineralization 21
Figure 12 - Carbonate inclusion in magnetite 22
Figure 13 - Quartz in magnetite 22
Figure 14 - Hydrothermally deposited magnetite 22
Figure 15 - Magnetite stringer in porphyry from drill core at Malå 23
Figure 16 - Syenitic, quarts depleted rock 23
Figure 17 - Granitic rock 23
Figure 18 - Hematite and syenite layering 24
Figure 19 - Tuff 24
Figure 20 - Mylonitizated porphyry 25
Figure 21 - from thin section 09 26
Figure 22 - Mechanically deformed crystal from thin section 03 26
Figure 23 - from thin section 13. Myrmekite 27
Figure 24 - from thin section 13. bent Carlsbad twin 27
Figure 25 - Fracture patterns 28
Figure 26 - Outcrops with the lake in the northwest 34
Figure 27 - Till cover close to main mineralization 35
Figure 28 - Northeast in the area with woods and heather looking at the central hill containing the mineralization 36

Figure 29 - Image locations..... 45

List of Tables

Table 1 – Drill-hole observations..... 13
Table 2 - Thin section list..... 16

Presentation of the Ekströmsberg mineralization

The Ekströmsberg mineralization

The Ekströmsberg mineralization is an iron ore deposit in the Kiruna area. Since GIAB took over the claim, there has been a need to verify previous work done there. This thesis is part of that verification process.

History and location

The earliest known printed reference to Ekströmsberg appear in a text by Abr. Romans written 1818 (Eriksson, 1904). In this text a certain 'Brukspatron Ekström' claims that he a few years earlier, with directions from local farmers, visited the iron mineralization. Ekström was of the opinion that the size of the mineralization surpassed that of Kiruna and Luossavaara, but despite this exaggeration it was not until 1895 that it was rediscovered and in the subsequent year made into a claim for the first time.

This mineralization is situated 30 km west of Kiruna (Figure 1).

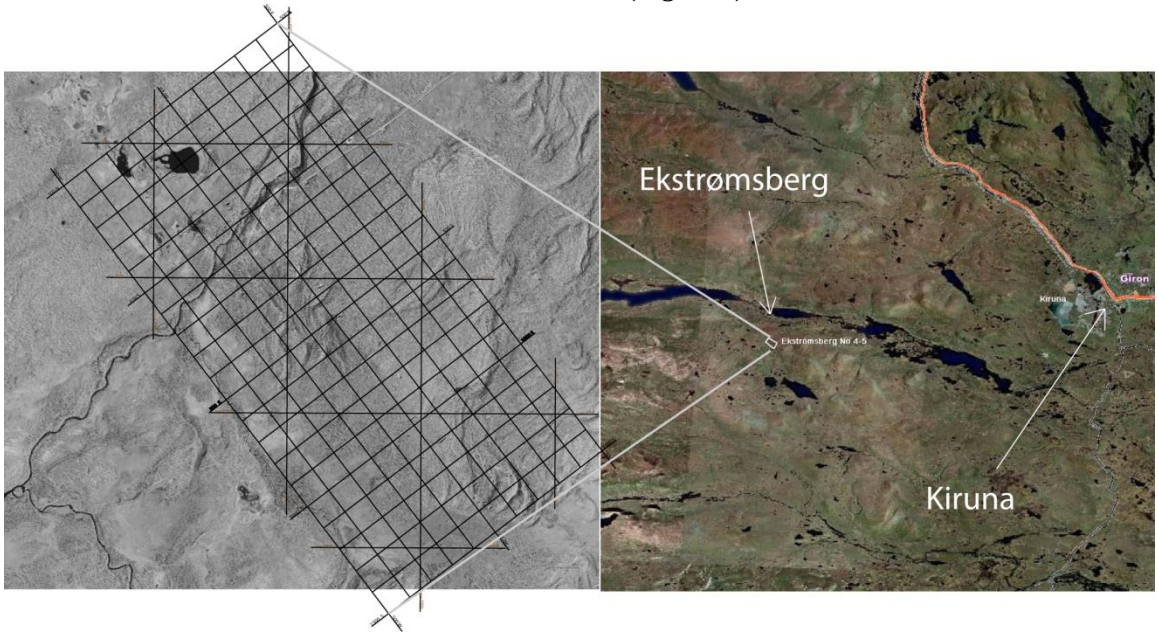

Figure 1 - Arial photo showing the town of Kiruna to the right and the surveyed area indicated by the arrow

In order to get to the site (Latitude: 67.801045, Longitude: 19.513289), one has to turn southwest of the road from Kiruna to Nikkaluokta, cross the 1 km wide lake Laukkusjärvi and then proceed by help of a terrain vehicle on the last 4 km of dirt road that was made by LKAB. Airlift by helicopter is also possible. The area of this survey, roughly between 585 m and 700 m above sea level, is a 2 km by 1 km rectangle (Figure 1) on the northwest sloping side of the mountain Piedjasjtåkka(1014m) This area is aligned over the main mineralization in a N325° direction. Most of the area is covered by glacial till. The find has been surveyed several times up through the 20th century. Activities included that pits were dug, 48 drill holes were made and test mining has been done. Several mapping and geophysical surveys have also been made as the claim has changed ownership. The most thorough survey took place in the period 1961 to 1969 (Frietsch et al. 1974) when most of the drilling was done.

Regional geological setting

The Baltic Shield has grown progressively during geological time from the north-eastern part, consisting of the Kola – Peninsula, Northern Norway and Karleen, down towards the south-eastern part of Norway It has grown through accretion and production of new crust near subduction zones, in

an island arc setting or continental shelf setting. The oldest Archaic bedrock extends south into Sweden. The Archaic Råstojäure gneiss complex is found just north of Kiruna. A smaller area of similar bedrock is also found at Sarrjärvi, 13 km southwest of Kiruna and has been dated to be about 2710 Ma. Svekokarelean granites, pegmatites, aplites and gabbro has intruded into the Archaic rock north of Kiruna. 1870 Ma perthitic granite belonging to the northern part of the Svecofennian province can also be found intruding the Archaic Råstojäure gneiss complex. The Svecofenninan and Lapponic bedrock is thought to have the older Archaic rock underneath it as far south as Jockmock (Lindström et al. 1991). The svekokarelean orogen's folding and metamorphosis occurred 1880 – 1800 Ma ago.

Local geological setting

The Ekströmsberg mineralization consists of several parallel lenses of varying thickness interbedded in mainly porphyry. The dip is vertical, and the iron mineralization is approximately 1400m long (Fagerberg et al. 1963). The investigated area is believed to be part of an anticline (Offerberg et al., 1967) and has evidently been subjected to various regional pressure regimes. Other rock types found within a 2 km range are granite in the east and syenite porphyry originating from the second phase of the Svecofennian orogeny (Bergman et al., 2001). A terrain description is provided in Appendix 1.

Suggested theories for genesis and deposition

There are two theories that have been suggested about the deposition of the Ekströmsberg deposit. Geijer (Geijer et al., 1974) and Frietsch (Frietsch, 1973) can be said to be the most prominent advocates of the magmatic differentiation model. In this model a (preferably alkali) magma chamber is differentiated under increased influence of volatiles, likely water. The alkali conditions and the increasing water supply will favor oxidation to first create magnetite and secondly hematite. Al though Frietsch (Frietsch, 1974) admits the Ekströmsberg mineralization deviates from the typical Kiruna type due to lack of connectivity between the mineralizations he includes it in the Kiruna-type group. The mineralizations are believed to have intruded as sills into an earlier extrusive quartz – bearing porphyry and syenite porphyry. The ore was first formed as magnetite and later partially oxidized to hematite, with martite as a transitioning hematite stage. The surrounding porphyry is also assumed to have been leached of iron through metasomatic alteration leaving sericite and quartz.

Parak (Parak, 1975a) is in agreement with Frietsch as far as the magmatic origin but believes the iron mineralizations to be deposited as lava in a marine setting. The apatite that is associated with the deposits is believed to come from organic sedimentation.

The co-occurrence of magnetite and hematite can be explained from an oxidizing reaction of primary magnetite (Fe_3O_4) to secondary hematite (Fe_2O_3) according to:

(1) $$4\ Fe_3O_4 + O_2 = 6\ Fe_2O_3$$

The four most important factors influencing this reaction are grain size, availability of reducing and oxidating agents, temperature and acidity (Frietsch, 1967). The grain size' influence is straight forward. Smaller grains give a higher combined surface area on which the reaction can start and therefore speeds up the reaction. If water is the source of oxygen for this reaction, then a buildup of the H_2 spatial pressure will win over the spatial pressure of O_2 and eventually halt the reaction and act as a reducing agent unless it is released or neutralized by an alkali solution from a component, like sulfides or graphite. If a ferro-silicate is available during oxidizing conditions the reaction (1) will be limited by the competing reactions of forming more magnetite rather than further oxidizing to form

hematite (Muller, 1961). Grunner (1930) proved the reaction (1) in a laboratory at temperatures as low as 260°C, and that it most likely occurs at lower temperatures but slows down to a practical standstill at normal atmospheric temperatures, explaining the occurrence of magnetite in the open. However, at temperatures above 1100°C the oxygen pressure in reaction (1) becomes comparatively higher that the oxygen pressure in equilibrium with pure water, halting the escape of oxygen into hematite. This is why magnetite is called the high temperature form.

Method

Field map

There were several purposes to the geological fieldwork in Ekströmsberg. First and foremost, the area was surveyed to get a correct geological map of the area taking extra care to map out the iron oxides; magnetite, hematite and martite, in detail. This was done in order for GIAB to confirm the economic potential of the mineralization. This map will then be used to assess the surface area that is covered by these three types of mineralizations. Another priority was to look in detail on mineralization in between and surrounding the iron oxides to see if they could reveal anything about how the iron minerals were deposited.

The geological survey was performed by the author. During three weeks all of the outcrops that could be found in this 2 square kilometer area was visited and described according to the following approach:

A GPS position was taken (or several in the case of a large outcrop). This included an X and Y position in the RT90 system and a height measurement (See appendix 2 for more details)

A preliminary decision was taken in the field on rock type. This was done by looking at it with a hand lens to decide the mineral composition. The hardness of the rock was tested by scratching it with steel of different hardness and the color of the scratch marks was noted. Tests samples for chemical and thin section analysis was also acquired using a geological hammer. The chemical samples were filed for later work and not included in this current report. The magnetization was tested using two magnets of different strength (Figure 2). Structure such as layering, grain size composition (porphyry texture), mylonitization and other alterations were also noted when discernible.

Figure 2 - Tools used in the field. Notebook, hammer, GPS, magnet (sticking to the side of the outcrop)

The strike of the stratification was noted using the GPS as a compass because a normal compass was useless in the strong magnetic field of the Ekströmsberg mineralizations. Dip was measured using a protractor against a string loaded with a weight. The GPS found the strike (bearing) when walking in a straight line in the direction of the strike. In the few occasions where a mountain top in the far horizon that previously was decided to be north could be seen, a double check was made lining up a regular protractor and reading the offset.

Strike and dip of fractures were also measured. See figure 3 next page. Fractures were arranged after dominance. Strike/Dip marked in black for main fractures and pink for secondary and tertiary fractures.

Pictures were taken of bedrock samples and of the bedrock area as a supplement to drawn sketches of the same.

Other features of interest was noted, like the moraine overlying much of the area.

The above approach was also applied to the mapping of the previously dug test pits, although in many cases no bedrock could be found.

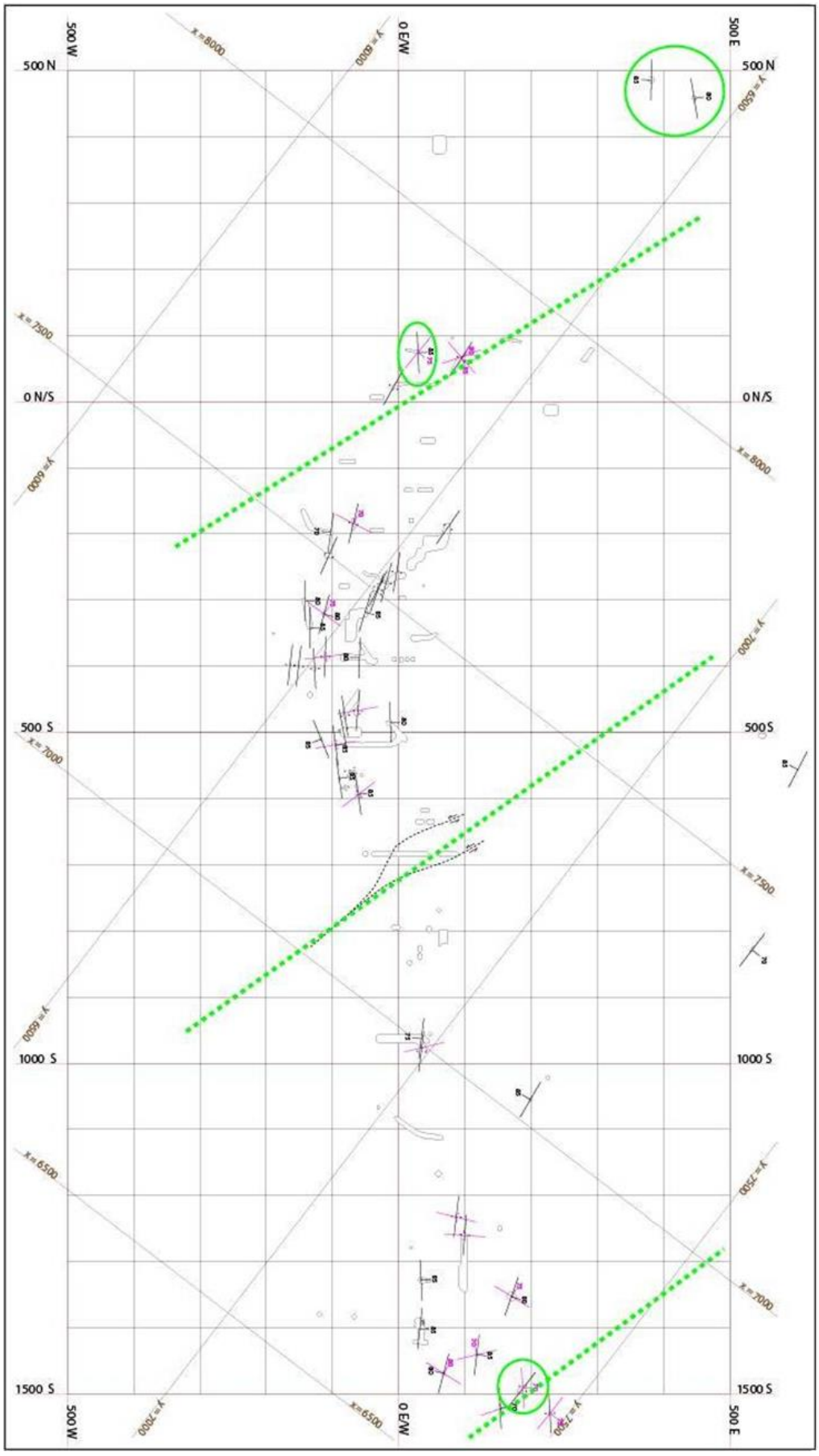

Figure 3 - Strike, dip and lager faults

Drill holes

The purpose of mapping out drill locations was to verify previous maps by Frietsch 1974.

This task of finding and noting down GPS position, altitude, trend and plunge of drill holes was done by all members involved in the project. Once one or two drill holes were found and identified, we used a previous map and compared our relative position on the GPS and just walked to where the next drill hole should be relative to the previous holes and looked around (Table 1). The drill location was typically marked by a steel casing/tube coming up about a meter from the ground. Trend was taken using the GPS and plunge using a protractor and a weight in a tread hanging from the tip of the steel casing. Trend measured in degrees relative to north, typically about 60 degrees.

Table 1 – Drill-hole observations

Drill hole	Altitude	Plunge	Trend		
66807	687	64			
66809	676	54	60		
5	671	56	60		
66806	674	46	60		
69802	669	50	50		
4	665	58	60		
67801	665	56	60		
69801	657	57	56		
69805	661			<_probable location	
66804	662	53	60		
6	658	57	60		
3	655	71	61		
66810	662	56	55		
67802				Not found	
68807	670	75	60		
65801	665	59	54		
65802	665	68	242		
67803	649	57	60		
66811	655	52	52		
7	656	56	51		
67808	644	68	50		
67805	632	62	55		
8	640	55	52		
66803	643	50	52		
2	625	63	52		
67804	625	55	42	?	
68802	619	64	55		
66802	632	48	50		
13	631	55	60		
66811	606	50	53		
68808	604	50	53		
15	602	57	60		
12	600	47	58		
68801	592	48	63		
68805	595	45	50		
68804	591		60	in the lake	
68805	586	59	58		

Malå drill core storage

We went to the Malå drill core storage to sample the iron mineralization (Figure 4) at depth, for chemical analysis and thin-section production. We also wanted to have a look at the fault zone (Figure 3) since the surface survey had revealed no visible faults. Another feature we hoped to find out was the angle to which the core had cut the layering at depth. Ahead of to the trip to Malå, Nordstrand and the author had through correspondence decided which cores we were to look at, but once we got there it turned out that even the updated drill-core list of remaining cores was in fact not up to date. This resulted in us not being able to have a look at the fracture zone cutting the main mineralization, since none of those cores are stored at Malå. On site we had to decide on what cores to sample. Four cores were sampled and logged. The samples we extracted were cut along the main axis of the core so that we would leave the entire length of the core intact.

Figure 4 - Magnetite core at Malå drill core storage

Thin sections

The sampling of bedrock and drill cores for thin-section analysis were mainly taken from the transition zone between the iron mineralization and the surrounding bedrock, with the aim of adding knowledge to the depositional environment of the iron oxides. Samples of apparent mylonitization was also taken to reveal structural shifts along the mineralization. Of 25 thin section suggestions 16 were returned and analysed. Locations of the thin sections are found in figure 5. A list of the thin sections is found in Table 2. The thin sections were analysed with a microscope. A general description containing minerals, grain size and general structure was done for each thin section, see appendix 3. Magnified pictures were taken of features of interest.

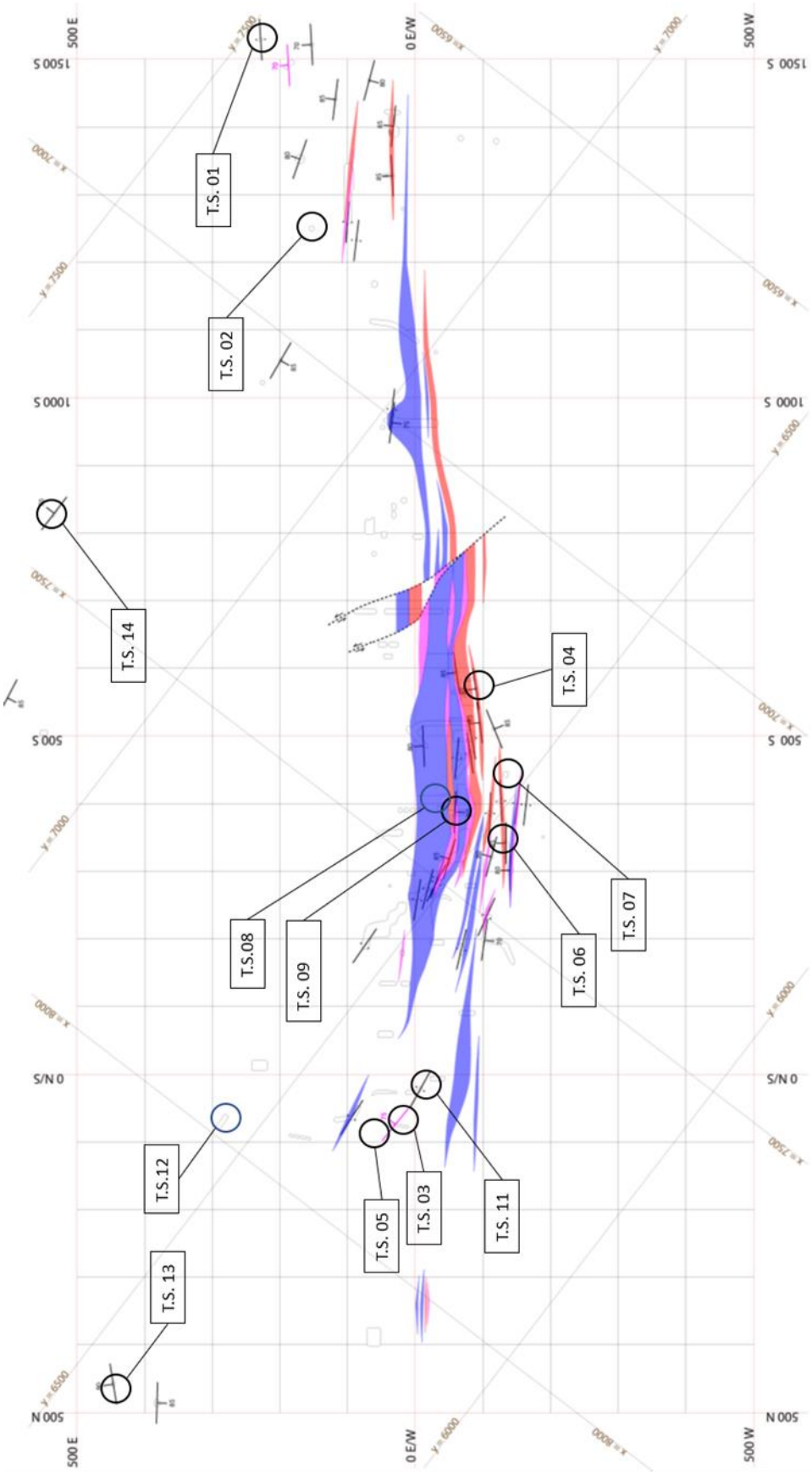

Figure 5 - Thin section location

Table 2 - Thin section list

Test name	Puck	Deliverd T.S.	Returned T.S.	New name
ebhl 60		x	x	T.S. 16
ebhl 21		x	x	T.S. 04
ebhl 20	x	x		
ebhl 29		x	x	T.S. 07
ebhl 45	x	x		
ebhl 54a		h	x	T.S. 01
ebhl 49		x	x	T.S. 13
ebhl 46		x	x	T.S. 12
ebhl 57		x	x	T.S. 14
ebhl 6		x	x	T.S. 02
ebhl 07	x	x		
ebhl 27	x	x	x	T.S. 06
ebhl 59		x		
ebhl 41		x		
ebhl 52		x	x	T.S. 05
ebhl 52b		x	x	T.S. 03
ebhl 48		x	x	T.S. 11
ebhl 38	x	x		
ebpg 12 2/3 öst		x		
ebpg 19 Hiö	x	x	x	T.S. 08
ebpg 35		x	x	T.S. 10
ebpg 19		x		
ebpg 19 Brevid Mag i öst		x	x	T.S. 09
BH 67804 69,5m	x	x	Drill hole	T.S. 15

Compiling of data and drill core projections

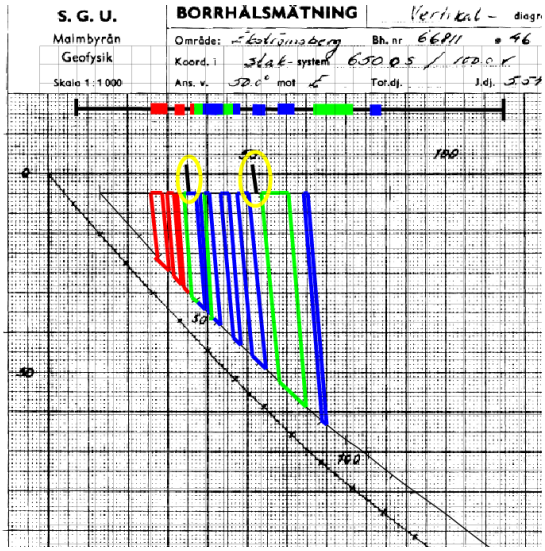

Figure 6 - Original drill hole protocol with offset and re-scaled interpretation on top. The yellow circles show plunge observed in area.

The software used to create maps, figures, text and edited pictures was Adobe Illustrator CS4, Acrobat reader, Microsoft Excel 2003 and Microsoft Word 2007.

When comparing my own logging of drill holes 69802, 67804, 68801 and 12, with the historic logging protocols of the same drill holes, I found a good correlation between them, and therefore decided to include several other drill holes when making my map. The aim was to make projections of all the relevant drill cores up to the surface in order to use them as supplements when compiling the final map. Most drill hole protocols provided a detailed profile that was used instead of my own drill hole plunge measurements made on site in Ekströmsberg. Each profile was copied and entered into its relevant vertical cross sections at the correct coordinates (Figure 6). The different iron mineralizations was

graphically entered onto the profile and then projected up to the surface. The drill holes used for this purpose is found in figure 7.

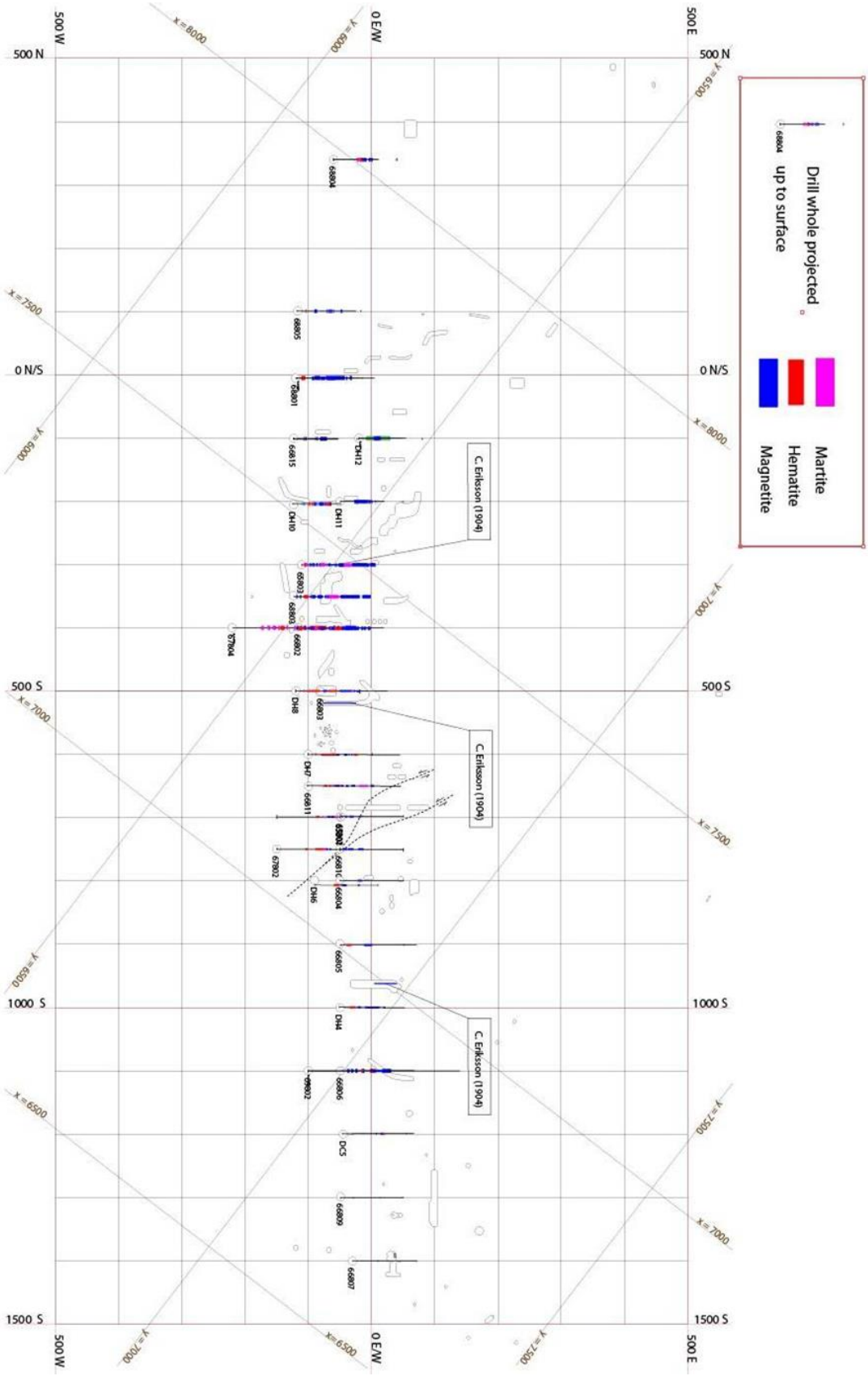

Figure 7 - Drill-hole projections

The parameters used for projecting the drill holes up to the horizontal surface profile were the surface dip observations made in the vicinity of the drill holes, the magnetic map (Nordstrand et al. 2009) and in those cases where several drill holes were entered into the same cross section the correlation between drill holes were also taken into account. These one-dimensional projections were later resized, pointed in the right trend, and entered on top of the field observation map (Figure 8).

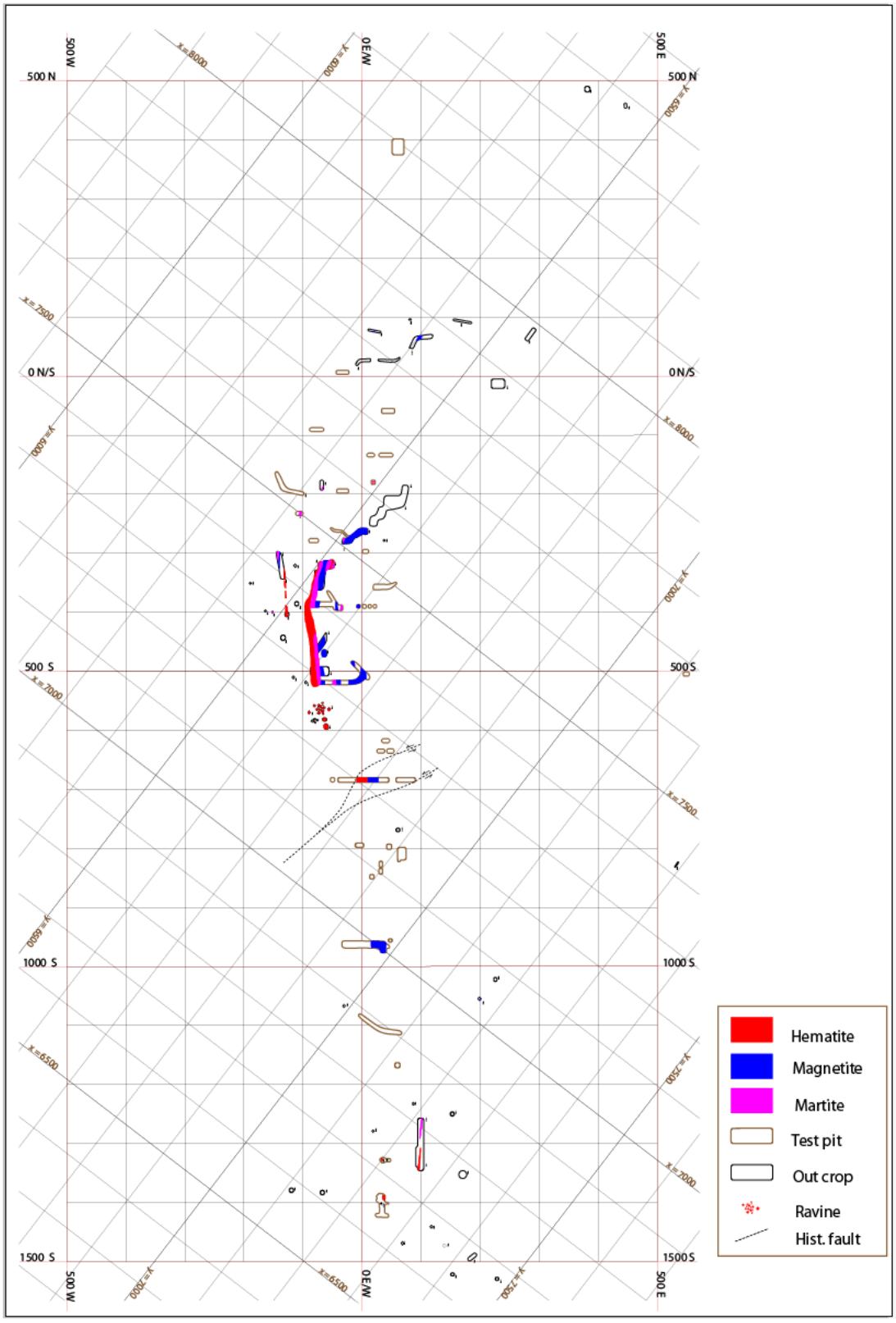

Figure 8 - Field observation map

The final map is a compilation of field observations including fracture patterns, strike and dip measurements, lithologic observations, drill-hole projections and some historic data. Each of these observations were put in separate layers in Adobe Illustrator and compiled to make the final map.

Historic drill-hole placement, logging and interpretation fits well with observations of the 4 cores that was logged at Malö. For this reason the historic logging and geometries have all been assumed to be good and used as input when compiling the final maps

Surface observations in the field also fit well with historic observations, but here the observed data constitute a complete coverage and have been used to make the final maps.

Thin sections have been used primarily to look for evidence of stess regimes. Mineral and chemical composition has not been a priority, which is also why the chemical samples have not been used for this thesis.

Data and map accuracy

The map outlining the iron mineralizations must be read with a few reservations in mind. There has not been any distinction made between low grade and high-grade concerning the iron content in the oxides. Primarily because most of the mineralization is observed to be high grade, which is supported by previous observations (Fritsch, 1974). The main body of the mineralization is interbedded with up to 10m thick cells or bands of nonferric lithology like quartz or syenite porphyry that are not included in the map, and based on field observations, as much as 20% of the main magnetite body's economic value can be discounted because of this. The smaller surrounding iron oxides and parallel observations are meant to be as accurate as possible.

I had no way of checking the drill-cores plunge at depth. I the end, my ambition to check the plunge of the drill-holes below the surface relative to other layers also turned out to be beyond what time allowed, when visiting Malå.

Exact compass readings were hard to achieve due to the compass not working properly in this area, however the overall conclusions should be valid due to the sheer number of observations stacking out single errors.

Drill-hole projections are rough estimates since correlation between all drill-holes and a detailed logging of available drill-cores was beyond this papers scope. For this reason, the projections made closest to the surface have been given more attention than the deep projections when compiling the final map.

The porphyry in the area is assumed to be a displacement of a deep-seated magma chamber. This should probably be better established in order to bring the depositional discussion forward.

Results and observations

Field observations

Outcrops were commonly found near the iron mineralizations. Most of the test pits had been dug perpendicular to the strike of the iron mineralizations but were dug relatively narrow and roughly 30 years prior to the fieldwork for this thesis. The test pits have now collapsed, and in most cases, nothing can be read from them since the bedrock has been covered over again. On each side of the outcrops of the main mineralization, till covers most of the bedrock. Throughout the surveyed area magnetite, hematite and the transitional martite, can be found in substantial quantities and have been mapped out in the field observation map (Figure 8). The main magnetite body consists of 10's of meters of pure homogeneous magnetite (Figure 4).

Figure 9 - Magnetite typical of Ekströmsberg

The hematite is easily distinguished by its red streak mark (Figure 10) and lack of a strong magnetic field. An overview of the mineralizations, outcrops and test pits are found in the final map on the next page (Figure 11).

Figure 10 - Hematite typical of Ekströmsberg

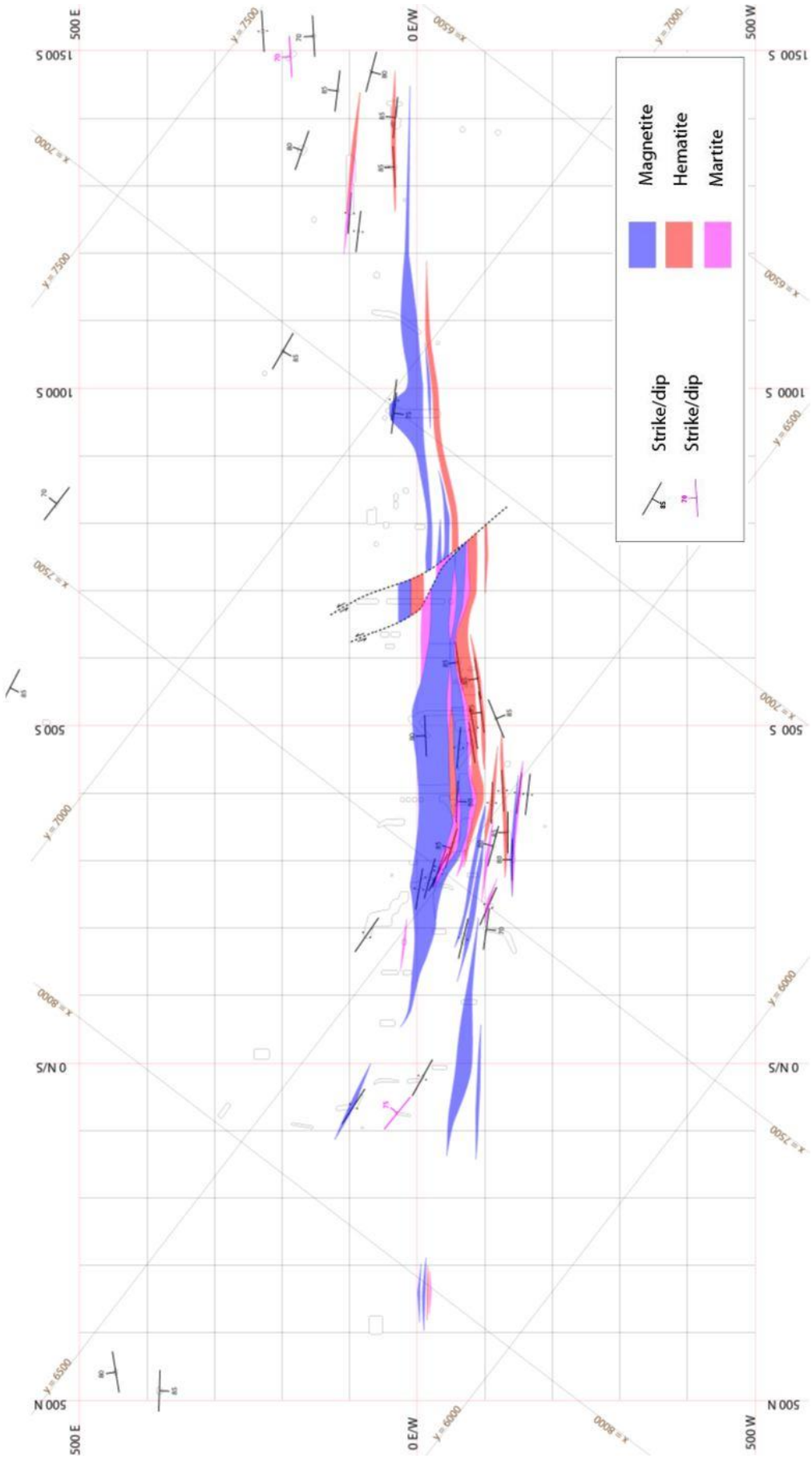

Figure 11 - Final Map of Ekströmsberg mineralization

An estimated 20% of the main magnetite body are in fact large lenses that contain quartz, various porphyry, carbonates or apatite inclusions in the magnetite (Figure 12, Figure 13).

Figure 12 - Carbonate inclusion in magnetite

Figure 13 - Quartz in magnetite

The main body of magnetite which is stratigraphically lower than the main hematite bodies to the southwest (Parak, 1975a), is the largest single body. Since this is the main economical target at Ekströmsberg this is also where the test mining pit can be found at about 50 meters west and 350 meters south in the local grid system. There are some clear cases of hydrothermal alteration of the magnetite (Figure 14) found as infill in the brecciated surrounding rocks

Figure 14 - Hydrothermally deposited magnetite

The melting temperature of dry magnetite is very high and an attempt to map out grain sizes in the surrounding rock in order to have an idea of the temperature gradient was conducted. The result of this was that no significant contact metamorphism was found anywhere at Ekströmsberg. No other conclusive sign of a temperature-induced pattern of the surrounding rock was found with distance away from the iron mineralization. Although far from absent, the limited control of observable adjacent rocks to the iron mineralization cannot exclude a larger temperature gradient hiding under the till cover. The hematite lenses, up to 10 meters thick, occur as elongated lenses either in conjunction with the magnetite or as separate parallel lenses with no apparent connectivity between them. Martite always make up a transitional zone between magnetite and the hematite when there is no other rock separating them. The bedrock in this transitional zone is otherwise hydrothermally altered porphyries of different composition (Figure 15).

Figure 15 - Magnetite stringer in porphyry from drill core at Malå

The quarts content varies greatly from almost nothing close to the iron mineralizations (Figure 16),

Figure 16 - Syenitic, quarts depleted rock

Figure 17 - Granitic rock

to the dominant mineral further away (Figure 17).

There is also finely layered rock of hematite and magnetite in the transition zones that stretch out parallel to the main mineralizations (Figure 18).

Figure 18 - Hematite and syenite layering

The largest area of outcrop is found close to the river. There it also becomes apparent that the iron mineralization is thinning out to only a couple of meters in thickness. In the southern part of the area the magnetite is mostly under the till, but an outcrop of a hematite lens is visible there and the supposed tuff (Figure 19) of Parak (Parak, 1975a) can be found here. This tuff was only found in two other places.

All three of these locations of tuff occur stratigraphically above an iron mineralization. It was not meaningful to sample the tuff due to severe weathering and hydrothermal alteration. If this really is an old ash layer or some other alteration like sericite is hard to say for the same reason.

Figure 19 - Tuff

When moving away from the main body, I did find samples of magnetite far from the main body, at times a hundred meters stratigraphically below it. But these were only centimetre thick observations. Often these magnetite stringers were not visible but were found by applying the magnet to a suspiciously protruding host rock, and if magnetic, knocking off a piece with the hammer. Several occurrences of thin magnetite with no apparent contact metamorphosis were found. I interpreted this as hydrothermally deposited magnetite coming up in a crack. One could argue that I had found the tip of another large body, but when checking against the magnetic field observations, there should not be any large magnetite body there.

Mylonitization (Figure 20) zones along the plates of hematite went on for over hundreds of meters, possibly more. This is indicative of a strike/slip process that has occurred along the observed mineralizations and there seem to have been ample supply of water available.

Figure 20 - Mylonitizated porphyry

Thin section observations

Descriptions of thin sections are found in appendix 3. Here, I present selected findings. The circled area in Figure 21 indicates a pressure shadow behind the rotating crystal. In more transpressional areas the surrounding matrix does follows the grains more closely.

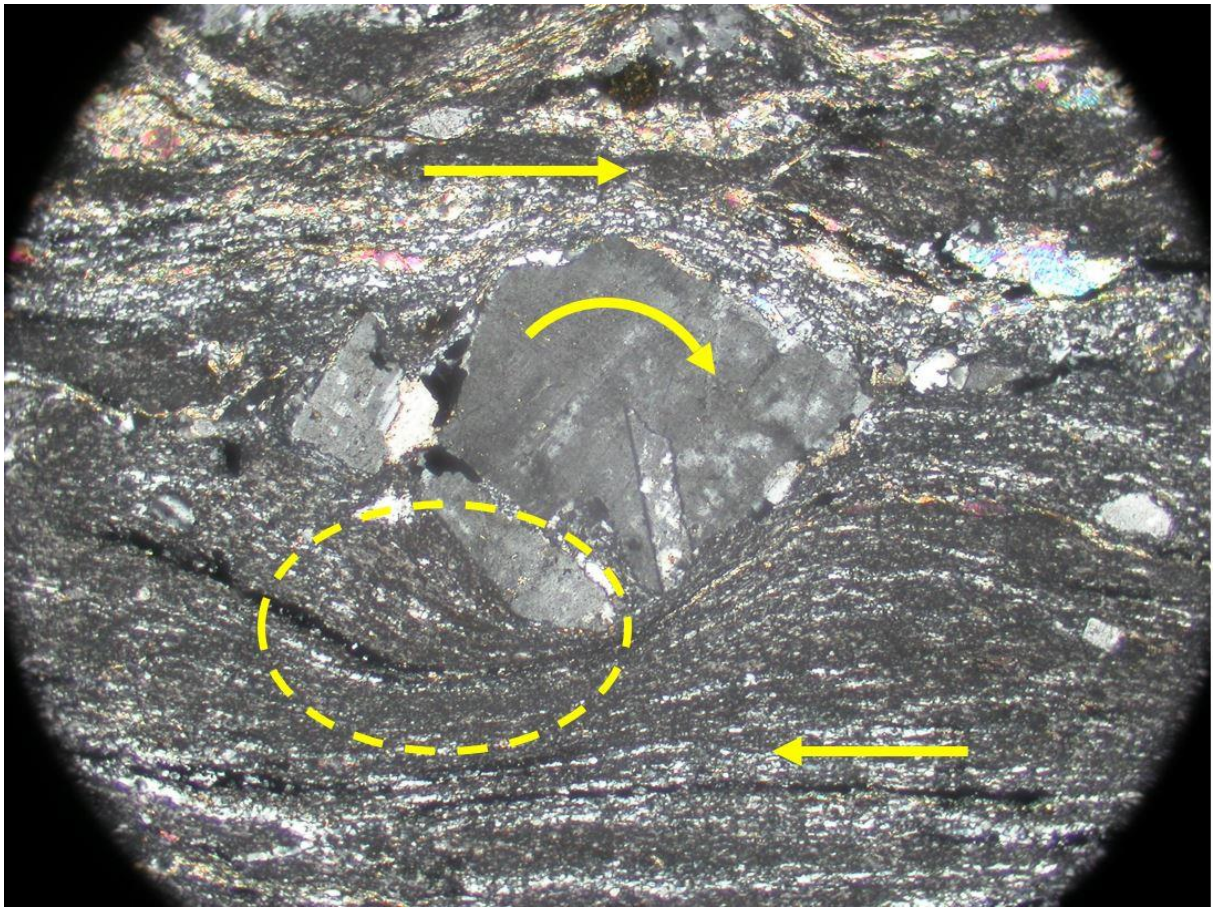

Figure 21 - from thin section 09

In Figure 22 one can observe that a piece of a feldspar crystal is broken off. Most likely a result of a combination of chemical weakening and then mechanical alteration in a transpressional setting. Figure 20 show the same mechanical alteration, but in that case the stretching and alteration of the crystals are apparent to the eye. Formation of mylonite is characteristic of moderately high temperature deformation.

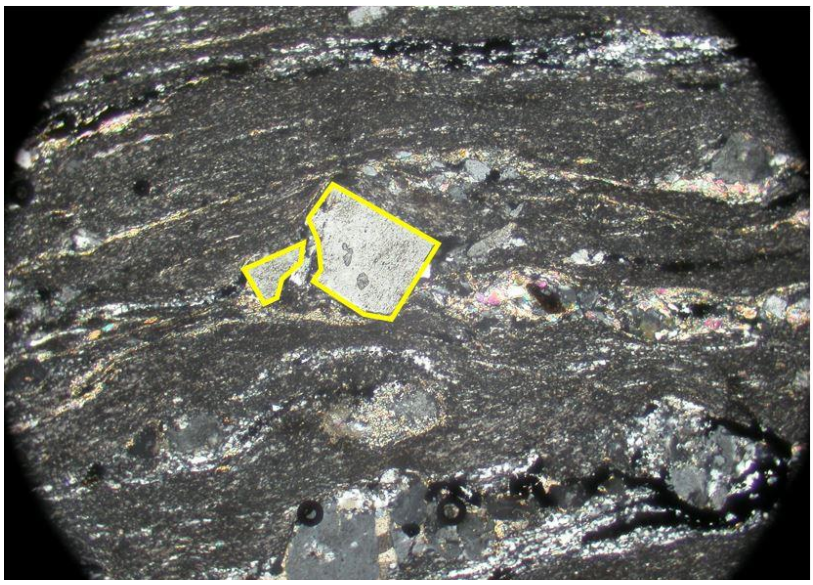

Figure 22 - Mechanically deformed crystal from thin section 03

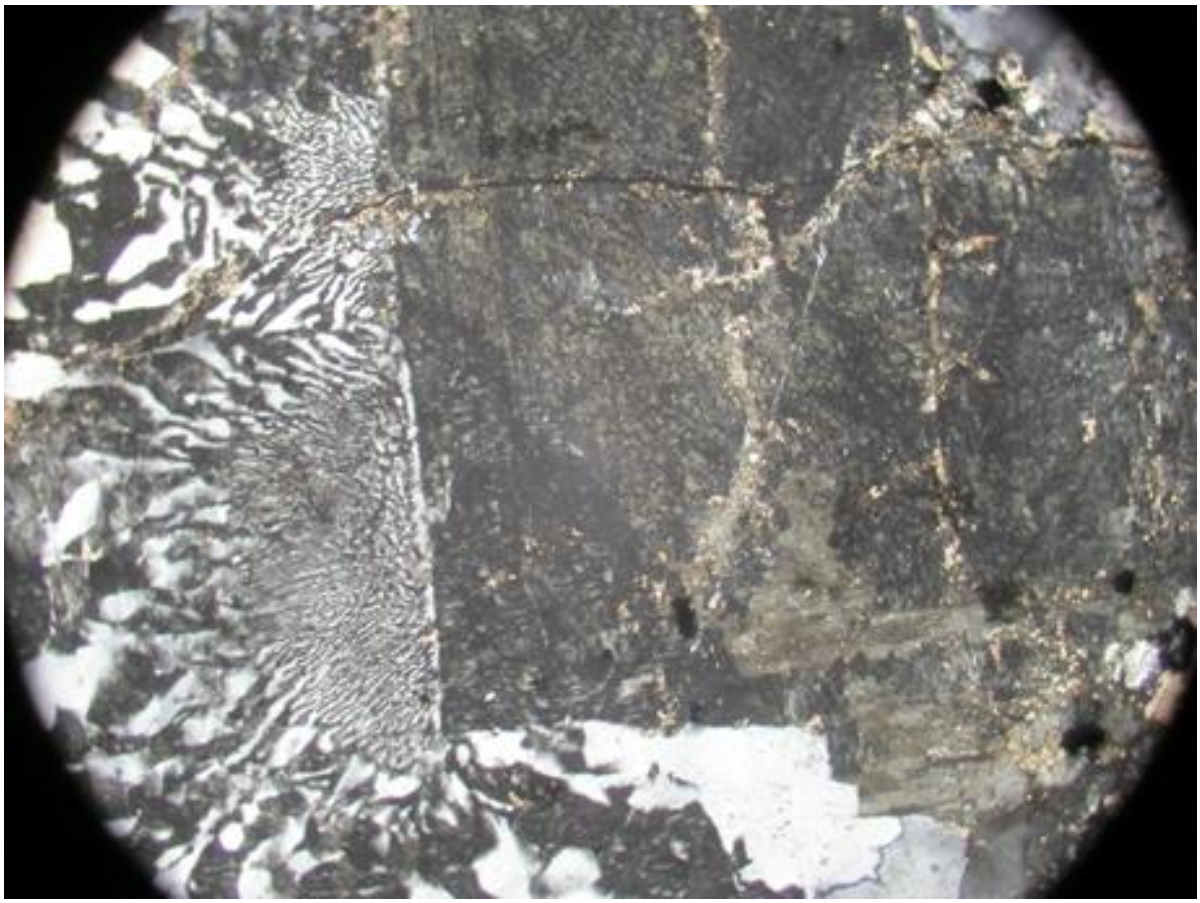

Figure 23 - from thin section 13. Myrmekite

Several cases of myrmekite texture were also found along the strike/slip zone. Myrmekite is here formed in albite with quartz intergrowth (Figure 23), most likely as a consequence of exsolution from the alkali feldspar during cooling, under conditions which silica was mobile in the rock. Its presence is also an indicator of a deformation processes. Another indicator of stress in the area is the appearance of bent Carlsbad twinning (Figure 24).

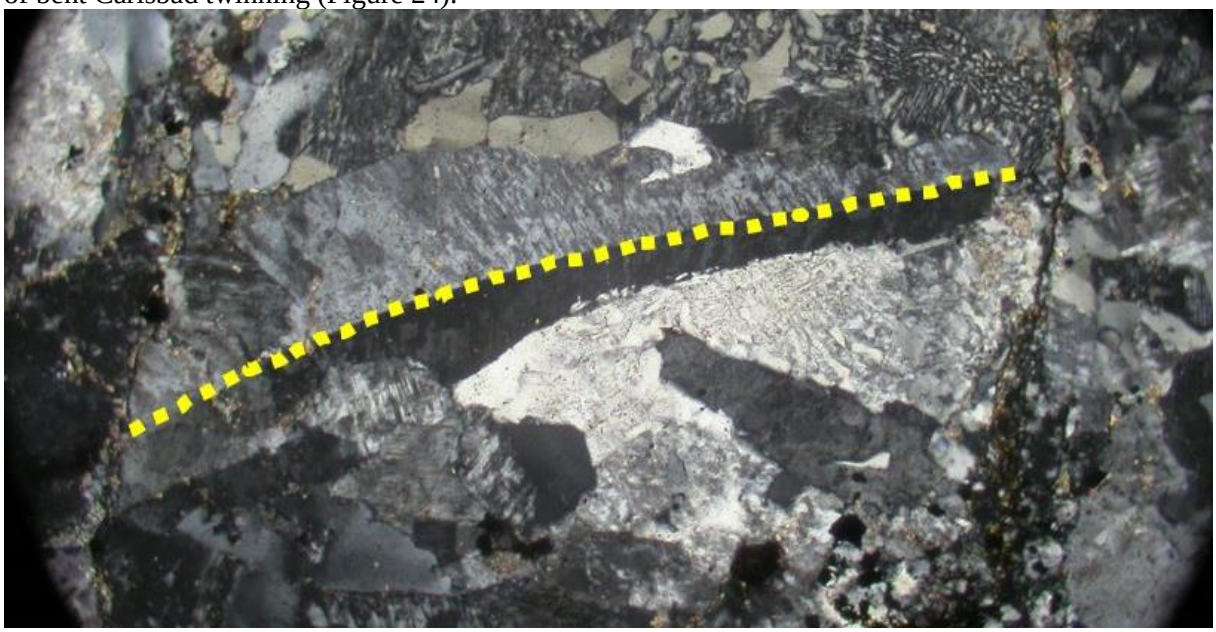

Figure 24 - from thin section 13. bent Carlsbad twin

Faults and fractures

The dip in the area show that this area has been overturned about 90° and the strike along the overall strike/slip fracturing is at about 325° (Figure 3). Secondary and tertiary fracture patterns are prominent (Figure 25 & Figure 18) and can be interpreted to be dominant in a few cases along the ends of the iron mineralization (green circles in Figure 3). The fractures in Figure 3 are graded after main fracture direction, coloured black, and secondary and tertiary directions in pink. Faults is coloured in stippled green.

What is important to remember is that there is a fourth fracture pattern not showing on the maps, the horizontal fractures. Horizontal fractures are observed over the entire area

.

Figure 25 - Fracture patterns

Malå drill core storage observations

The eight hour we had in Malå was spent looking at four drill cores (69802, 67804,68801 and 12). We logged the iron mineralization and were able to verify the validity of the historic drill core logs. One observation that was made while observing one of the drill cores was a faint cyclic colour pattern covering the magnetite. The pattern crossed the different drill core cases in a way that excluded any late external influence. The pattern was only repeated twice, like this: (dark grey, greenish, grey, dark grey, greenish, grey).

Discussion

When looking at the collected data one can find several arguments against and for either (1) the magmatic sill intrusion hypothesis, (2) the marine lava hypothesis or a (3) hydrothermal formational hypotheses.

If these mineralizations are intrusive sills then we would expect to see some kind of contact metamorphosis in the surrounding bedrock, and the reason for that is that a magmatic magnetite is very hot, and the surrounding porphyry bedrock is expected to be relatively cold. The porphyry is in itself an indicator of a rapidly cooled magma, making it unlikely that the deposition of a later, most likely much warmer magmatic iron mineralization happened in a deep (warm) setting with a stable temperature gradient, required for no contact metamorphosis. For this to happen the deposition of a magmatic magnetite would have had to be a much later event than the deposition of the porphyry, when everything has been re-buried, re-heated, and then subsequently intruded by a magnetite so saturated with water that it would be viscous and still not hot enough to re-melt the porphyry. Another, less fancy full, yet still somewhat unlikely scenario for an intrusive sill, or dike in an overturned sequence, is the argument that the mylonitization and layering has erased any trace of the contact metamorphosis, see Figure 18. The reason also this scenario is unlikely is the number of observations of the mineralization and surrounding rocks, without any contact metamorphosis. Especially the outlying centimetre thick magnetite stringers, does not look like a secondary re-deposition and lack both contact metamorphosis and mylonitization.

The marine lava depositional model is supported by the occurrences of the many long lenses of mineralization without visible connectivity at the surface. There are examples of iron mineralization transitioning seamlessly from magnetite to martite and hematite. It is entirely possible that all the plates connect at greater dept or had connected above prior to a possible erosional episode. Another possible argument for the magnetite reaching the surface, that is the seabed, as lava, is the cyclic pattern observed in Malå indicating a first, second and third phase of expulsion from a slightly differentiated magma chamber followed by a repeat of this. However, the cyclic pattern could have other explanations. The tuff (Parak, T., 1975), found stratigraphically above the mineralization sheds no light on the genesis of the mineralization. If this indeed is tuff, it is a natural weakness in the bedrock and thereby a way for intrusion or hydrothermal migration.

A regular hydrothermal deposition is supported by the fact that there is no contact metamorphosis. The presence of porphyry in this geological setting is probably a good indicator of rifting, which provides this case with a deep-seated heat source. A typical heat engine would fit, with meteoric water coming in from the sides to be heated to supercritical water, which then picks up the iron and deposits it as the water rises and temperature comes down again. The water then turns outward and sinks down to complete the cycle. Another source for water could be the subducted sea bottom that came down with the underlying Archean plate. There is ample proof of hydrothermal alteration in the surrounding bedrock, which in itself is no proof of hydrothermal deposition of the main mineralization. A heat engine could have continued to push water up through this rift and re-deposited some of the iron mineralization, but without adding to the total volume. Clear indication of hydrothermal alteration is found, and this might certainly be a secondary process, taking place after a magmatic deposition, but the opposite scenario is also likely. In such a scenario hydrothermally deposited iron mineralizations, still water wet, could be smeared out and intermingle with the host rock.

The main fault described by (Frietsch, 1974) crosses the main mineralization. At equal length to the south and north, the main strike of the bedrock, which is mostly around 330/130 degrees (See Appendix 2 for complete list of observations), turns away to the north/south, and a secondary fracture patterns in this direction becomes dominating (Figure 3. see green circles). It appears that in the north where the river crosses the main body, forces produced a more ductile deformation just as it has in the south. But the main magnetite body has resisted theses forces long enough for it to come to a clean break in a regular fault. Even further to the south and north the strike line up with the mineralization again. This could be interpreted to say that the deposition of the magnetite body was fast enough to

resist ductile deformation at the thickest part, yet hot enough for ductile deformation where the mineralization was thinner.

The stress regime in the area is dominated by these two directions, see figure 3, along the overturned strata and mineralization in a direction of about 330 degrees, and the secondary fractures at 60 degrees offset at about a 30 degrees direction and are quite prominent, even dominant in some areas. Rather than seeing these two fracturing directions as competing or separated in time from different stress regimes, evidence could be interpreted to hide a stress regime directed in between the two, close to straight north/south. One could argue that stratification in the overturned strata allows for easier fracturing along 330 degrees and consequently mask the true stress regime in the area. As the 330 degrees component is continuously compensated for by microfractures and ductile deformation over time, the 30 degrees component builds up stress, until it is dominant and eventually comes to a violent rupture, creating the main fault in the mineralization and the fault the river came down in (See green dotted lines in Figure 3). This fits with the observed mylonitization along the 330 degrees direction, and the lack of it in the secondary 30 degrees direction, since the 30 degrees direction in not so ductile, or ductile at all.

The horizontal fracturing is without observable large shifts; none were observed in Malå. Rather the horizontal fractures are made up by many smaller fractures separated by decimetres to a couple of meters. It is likely this is related to Offenbergs (Offerberg et al., 1967) anticline theory of the area, or may be due to exfoliation close to the surface.

Conclusions

- The iron mineralization likely was deposited after overturning of the strata, as a dike, hydrothermally, or possibly as a very wet magma. Either way a lot of water was involved.
- This mineralization never reached the surface. There are thin (1 cm) layers, often far from the main mineralization stratigraphically, also there is no contact metamorphosis, and no bubbles.
- It is possible the porphyry was deposited as a dike as well, after the overturning of the strata, but before the iron mineralization. This is because porphyry only becomes porphyry once it cools down significantly and rapidly from high temperature, which means it needs to travel up and not sideways.
- The stress regime goes straight north/south, but the stratification in the area makes it swing gradually from north/south out to 30 degrees and jump back to north/south again.
- A suggested next step in developing the depositional model would be to date the mineralization and its surrounding host rock.

Works cited

Ericsson, C., 1904. *Rapport över resultat av undersökning vid fyndigheter i Norrbottens län.* Manuscript, Kgl. Kommerskoll., page 13-28.

Frietsch, R., Nylund, B., & Oldeberg, H. (1974). *Ekströmsbergs Järnmalmsfyndighet - Rapport rörande resultaten av SGU 1961-1969.* Report, Sveriges Geologiska Undersökning Malmbyrån

Lindström, M., Lundquist, J., & Lundquist, T. (1991). Sveriges geologi från urtid till nutid *Studentlitteratur, Lund*. 491 p.

Fagerberg, B., Ornstein, H., 1963. *Borrkärnegods från Ekströmsberg.Makroskopisk kartering ur anrikningsteknisk synvinkel.* Report, Sveriges Geologiska Undersökning Malmbyrån

Offerberg, J., Werner, S., 1967. *Beskrivning till Berggrundskarbladen Kiruna NV, NO, SV, SO. Sveriges Geologiska Undersökning AF 1-4*. Survey.

Bergman, S., Kübler, L., Martinsson, O., 2001. *Description of regional geological maps of northern Norrbotten County (east of the Caledonian orogen).* Geological Survey of Sweden, Ba 56. Uppsala.

Geijer, P., Ödman, O. H., 1974. *The emplacement of the Kiruna iron ores and related deposits*. Survey. Sveriges Geologiska Undersökning. Serie C, nr. 700

Frietsch, R., 1973. *The Origin of the Kiruna iron ores.* Geologiska Föreningen. Stockholm, Förh., v. 95, page 375-380.

Frietsch, R., 1974. *The Ekströmsberg iron ore deposit, northern Sweden.* Sveriges Geologiska Undersökning. Stockholm. Serie C. nr. 708.

Parak, T., 1975a, *The origin of the Kiruna iron ores.* Sveriges Geologiska Undersökning. Stockholm. Serie C nr. 709

Frietsch, R., 1967. *The relationship between Magnetite and Hematite in the iron ores of the Kiruna type and some other iron ore types.* Sveriges Geologiska Undersökning. Stockholm. Serie C nr. 625

Mueller, R., F., 1961. *Oxidation in high temperature petrogenesis*. American Journal of Science. 259, pages 460 – 480.

Gruner, J., W., 1930. *Hydrothermal oxidation and leaching experiments; their bearing on the origin of Lake Superior hematite – limonite ores.* Economical Geology 25, pages 697 – 719.

Nordstrand, J., Sundqvist, F., 2009. *Geophysical modelling of Ekströmsbergs iron mineralization.* Examensarbete, Berg- och mineralteknik nr. E3794.

Appendix 1 – 5

Appendix 1: Area description

The river Rateksjåkk cuts the northwestern part from the rest of the area. This northwestern part contains a small lake with surrounding marshes, which is drained into the river Rateksjåkk. The rest of this northwestern part is vegetated by trees and the terrain is not easily traveled, particularly down by the river. Access from the southern side of the river is by a roundtrip of 3km on dirt roads. Immediately southeast of the river Rateksjåkk the terrain remains well vegetated, and, in some places, steep ravines can be found, particularly down to the river, however the western part towards the south is flatter and more marsh like, with smaller underbrush. When coming from the northwest towards the middle of the area the terrain rises, and this is also where the main mineralization can be seen in the open.

Figure 26 - Outcrops with the lake in the northwest

It is found northwest of the hill and along the southwest side of the hill. Where the mineralization and bedrock in general is found the terrain is rugged and mostly aligned along the strike of the mineralization (Figure 26). When traversing this area, one must be prepared for several ups and downs of up to 5 meters overlaying the general lay of the land. Large areas of rounded boulders can also be found here (Figure 27). They have not been mapped but are rounded and surprisingly well sorted when they appear, ranging in size from ½ meter to 2 meters depending on location.

Figure 27 - Till cover close to main mineralization

These areas of rounded boulders appear from the middle of the survey area and towards the south, and the larger fractions tend to gather in dips of the terrain. At the summit of the central hill the vegetation consists mainly of dwarfed birch. Vegetation is denser on the sunny southwestern side and restricts the view. Further along the ridge of the hill towards the south, the ridge itself actually decline by a few meters, while the terrain northeast builds up fast to form a less pronounced ridge towards the east. Halfway to the southeastern part of the area, magnetite bedrock is observed and can be said to mark the southern end of the central hill. All though it is fairly flat from this magnetite outcrop and 200 m towards the southeast, the water divide seems to follow the main mineralization. To the far southwestern side it is still decidedly lower topographically and near the southwestern edge vegetation is partly dominated by wet terrain without trees.

At the most southeastern part of the area the terrain again rises (also in the western part) and the vegetation is gradually reduced to consist mainly of heather with trees only in the lower west (Figure 28).

Figure 28 - Northeast in the area with woods and heather looking at the central hill containing the mineralization

Several curved incisions with boulder infill are found here resembling retreating end-moraines that have pushed up against the mountain. The boulders have either been from the moraine or dumped on the terrain as the ice retreated. Due to the fact that during the survey only a single somewhat rounded magnetite boulder (½ m) was noted at about 50 meters east of the main body of the mineralization, the moraine covering the area is most likely a top-moraine. This would go a long way of explaining why no trails of magnetite boulders can be found. They are there, but under the moraine. A feature similar to the end-moraines in the southeast can be found to the east where a circular slide is found. Water can be seen coming up from the ground in the middle of this. This circular slide observation sets the end-moraine theory on less firm ground because of their similar features. The end-moraine also seems to coincide with fractures in the terrain in some cases. Since these features are of limited importance for this paper the end-moraine theory will have to do.

In connection with Ericsson's (Erikson, C., 1904.) mapping of the area several large pits where dug. They can all be found today but only a few have not caved in completely and can be used to observe the bedrock. The drill sites are also accounted for.

Appendix 2: field observations with coordinates and fractures

Name	x coordinate	y coordinate	Altitude	Strike	Dip	Fracture Strike	Frac. Dip	Frac. Str. 2nd	Frac. Di 2nd
Loc1	7285	6591	640	102	85				
Loc2	7245	6604	649						
Loc3	7259	6629	640	105	85				
Loc4	7268	6640	643	312	85	15			
Loc5	7275	6645	646	310	85	15	85		
Loc6				302	90	15	85		
Loc7	7294	6674	652						
Loc8	6654	7247	694	160	90				
Dike2	6719	7194	681						
Häll1	6750	7245	688						
Dike3	6906	7089	674						
Häll2	6818	7216	678	145	90	230			
Häll3	7500	6425	616	165	90				
Häll4	7500	6523	624	158					
Häll4(2)	7542	6528	621	150	90				
Häll5	7595	6525	613						
Häll6	7594	6449	613						
Ebhl01	6658	7246	690	330	85				
Ebhl02	6643	7317	699	157	80	260	80		
Ebhl03	6675	7339	696	330	85	220	70		
Ebhl04	6766	7368	712						
Ebhl05	6778	7324	693			340	80	260	75
Ebhl06	6848	7250	681						
Ebhl07	6816	7215	679			145	90	235	90
Ebhl08	6745	7257	689						
Ebhl09	6829	7178	674	330	90	65	90		
Ebhl10	6586	7107	679						
Ebhl11	6612	7156	684						
Ebhl12	6723	7195	682	320	85				
Ebhl13	6746	7159	679						
Ebhl14	6885	6989	669						
Ebpg04	6905	7093	674						
Ebpg04(2)	6892	7024	673						
Ebpg03	6859	7125	674						
Ebhl15	7072	7162	659						
Ebhl16	6896	6959	666						
Ebpg05	7006	6981	669	150	75	40	90		
Ebbl01	7184	7129	673						
Ebhl17	7269	6942	659						
Ebbl02	7209	6890	682						
Ebhl18	7181	6879	678						
Ebpg07	7144	6913	675						
Ebpg08	7146	6887	676						
Ebpg06	7091	6894	672						
Ebpg09	7109	6900	674						
Ebhl19	7093	6639	640						
Ebpg10	7114	6847	663						
Ebpg11	7173	6743	660						

Ebpg12	7240	6818	670						
Ebpg12(2)	7213	6802	684						
Ebpg13	7262	6856	664						
Ebbl03	7344	6880	654						
Ebbl04	7295	6806	671						
Ebpg17	7269	6793	670						
Ebpg15	7250	6770	672						
Ebpg16	7278	6761	668						
Ebhl20	7239	6685	655	315	85				
Ebhl21	7246	6644	640	315	85				
Ebhl22	7271	6662	640						
Ebhl23	7270	6581	639	120	85				
Ebhl24	7283	6606	642	315	85	40	90		
Ebpg18	7290	6617	643						
Ebpg18(häll)	7361	6671	653						
Ebpg18(häll2)	7362	6643	647	320	80				
Ebhl25	7329	6598	641	315	90				
Ebhl25(pos2)	7374	6583							
Ebhl26	7424	6434	614	325	80				
Ebhl27	7393	6470	622	325	85				
Ebhl28	7352	6516	638	320	90				
Ebhl29	7313	6524	630						
Ebbl04	7311	6464	616						
Ebhl30	7331	6475	617	330	90				
Ebhl31	7346	6480	619	330	90				
Ebhl32	7306	6597	644	130	90				
Ebhl33	7348	6597	641	145	90	40			
Ebdh66802	7379	6531	630						
Ebhl34	7382	6513	629	335	90	42	90		
Ebpg19	7406	6566	633	142	80				
Noll400s	7445	6624	634						
Ebbl05	7379	6427	625						
Ebhl35	7355	6433	626						
Ebbl06	7276	6353	617						
Ebbl07	7438	6349	609						
Ebpg27	7533	6353	609						
Ebhl36	7531	6411	611	150	70				
Ebpg26	7502	6426	614						
Ebpg25	7478	6471	624						
Ebhl37	7422	6467	624	340	80	270	75		
Ebhl38	7465	6525	625	343	85				
Ebhl39	7398	6532	630						
Ebpg21	7505	6633	630						
Ebmylonit	7356	6508	628						
Ebpg24	7513	6476	621						
Ebpg24(2)	7525	6527	620	340	90				
Ebhl40	7502	6520	624	350	90				
Ebhl41	7548	6537	622						
Ebpg23	7522	6549	628						
Ebhl42	7648	6539	610	355	90				
Ebhl43a	7618	6546	611						
Ebhl43b	7557	6465	616						

Ebhl44	7557	6429	608	337	90	260	70		
Ebpg28	7566	6450	610						
Ebpg29	7529	6523	612						
Ebpg30	7620	6488	607						
Ebpg31	7648	6455	608						
Ebpg40	7728	6431	598						
Ebpg32	7678	6485	605						
Ebpg33	7627	6356	598						
Ebhl45	7842	6395	567	40	85	355	90	280	80
Ebhl45b	7875	6417	567						
Ebhl46	7962	6548	580						
Ebhl47	7690	6277	587						
Ebpg34	7727	6327							
Ebhl48	7760	6342	585	350	90				
EbRplats	7888	6552	589						
Ebhl49	8378	6440	571	315	80				
Ebhl50	7921	6447	580						
Ebhl51	7870	6364							
Ebhl52	7824	6335	582	0	75	320	85		
Ebhl53	8360	6383	578	140	85				
Ebpg35	8087	6183	598						
Ebhl54	6676	7470	709	320	90	0	75		
Ebhl55	6641	7410	702	320	90	35	90		
Ebhl56	6678	7421	705	320	70	0	90		
Ebhl57	7414	7292	655	0	70				
Ebhl58	7035	7167	672	170	85				
Ebhl59	6993	6990		325	90				
Ebhl60	7687	7195	627	350	90				
Ebpg39	7684	7103	623						
Ebhl61	8014	7460	605	325	90	210	80		

Appendix 3: Thin section description

T.S. 01: Red stained, foliated feldspar porphyry.

Groundmass: Quartz, feldspar, muscovite

Accessory : Chlorite, epidote

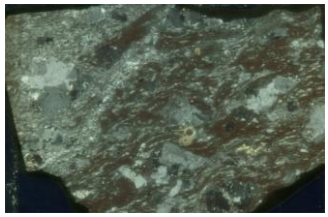

T.S. 02: Red stained granophyre.

Groundmass: Quartz, albite, muscovite, K-feldspar

Accessory : Titanite, calcite

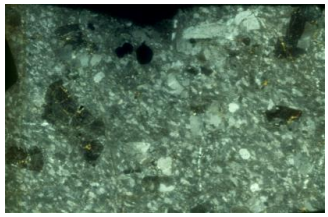

T.S. 03: Red stained K-feldspar porphyry

Groundmass: Quartz, chlorite, muscovite, K-feldspar

Accessory : Titanite, calcite

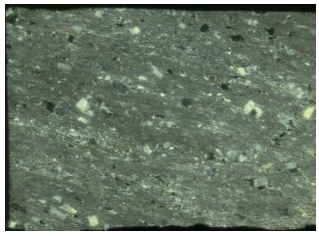

T.S. 04: Red stained mylonitizated Quartz-feldspar porphyry.

Phenocrysts flattened and elongated.

Groundmass: Quartz, chlorite, muscovite, feldspar, biotite

Accessory : Apatite

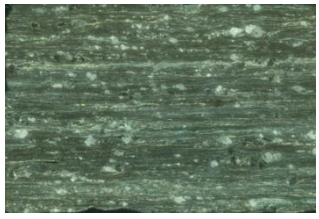

T.S. 05: Opaque banded quartz-feldspar-biotite

Meta tuffite with foliation.

Phenocrysts of Quartz and feldspar

Groundmass: Quartz, chlorite, muscovite, feldspar, biotite

Accessory : Apatite, coarse grained on the sides.

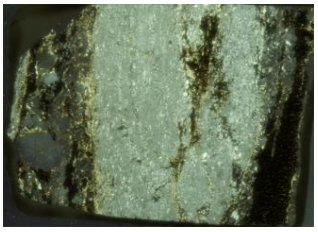

T.S. 06: Opaque disseminated Quartz porphyry.

Biotite partly replaced by chlorite.

Groundmass: Fine grained quartz, muscovite, K-feldspar, plagioclase, biotite

Accessory : Apatite, chlorite

T.S. 07: Feldspar porphyry with K-feldspar phenocrysts.

Foliation through schlieric orientation of matrix.

Finely distributed magnetite and hematite.

Groundmass: Fine grained quartz, muscovite, feldspar, biotite.

Accessory : chlorite, titanite.

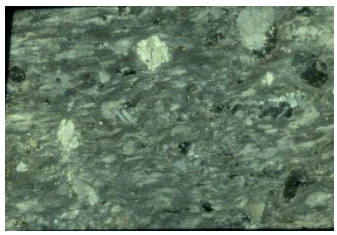

T.S. 08: Deformed Quartz and feldspar phenocrysts

Mylonite. Foliation by elongated Quartz fragments

And parallel orientation of biotite and muscovite

Groundmass: Quartz, albite, muscovite, K- feldspar, biotite

Accessory : Apatite, Chlorite replacing biotite, magnetite

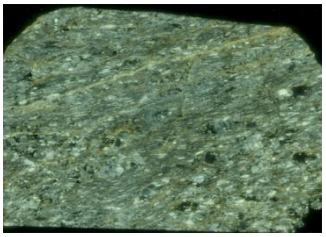

T.S. 09: Red stained felsic mylonite. Long elongated quartz lenses show undulous extinction. Micro shear zones consists of quartz, feldspar and chlorite.

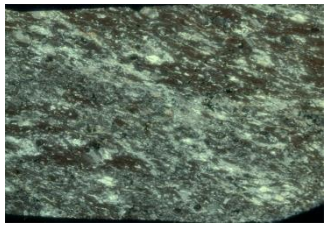

Groundmass: Quartz, feldspar, chlorite

Accessory : Calcite, titanite.

T.S 10: Well foliated quartz porphyry.

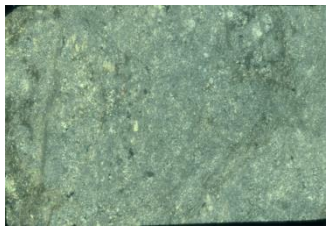

Groundmass: Quartz, plagioclase, K- feldspar, muscovite, Opaque

T.S. 11: Well foliated K-feldspar. Porphyry

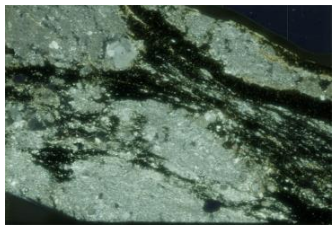

Groundmass: Quartz, K- feldspar, biotite, opaque, plagioclase

Accessory : Chlorite, muscovite

T.S. 12: Red stained granophyre

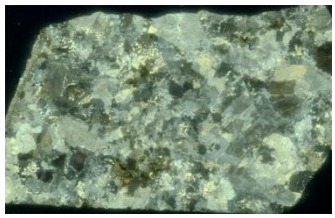

Groundmass: Quartz, albite, muscovite, K- feldspar

Accessory : Chlorite, opaque, calcite, titanite

T.S. 13: Granophyre. Plagioclase probably abitiziced under formation of excess calcite

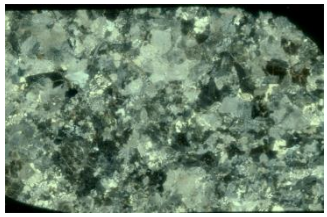

Groundmass: Quartz, albite, muscovite, K- feldspar

Accessory : Chlorite, opaque, calcite, titanite

T.S. 14: Opaque-disseminated quartz porphyry. Biotite partly replaced by chlorite. Micro fractures with quartz, feldspar, muscovite and biotite.

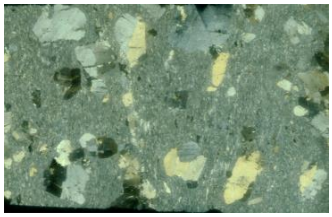

Groundmass: Fine grained quartz, K-feldspar, biotite, muscovite, plagioclase

Accessory : Apatite

T.S. 15: Red stained, extremely foliated (mylonitizated) feldspar porphyry. Extremely sericitized and carbonized.

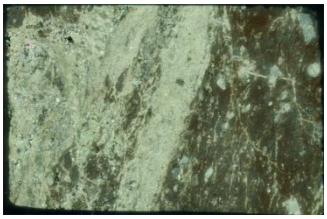

Groundmass: Quartz, feldspar, opaque

Accessory : Chlorite

T.S. 16: K-feldspar porphyry. Micro fractures with calcite.

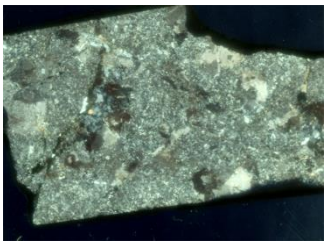

Groundmass: Quartz, K- feldspar, opaque, biotite

Accessory : Apatite, chlorite, calcite, zircon, epidote.

Appendix 4: chemical test samples

ebhl 54a
ebhl 49
ebhl 27
ebhl 46
ebhl 07
ebhl 45
ebhl 20
ebhl 41
ebhl 57
ebhl 39
ebhl 6
ebhl 60
ebpg 19 Next to Mag. in east
eb pg 12 2/3 east
ebpg 19 corner
BH 67804 342m
BH 68801 97,5m
BH 69802 145m
BH 67802 171m
BH 68801 141,5m
BH 67804 274m
DH 12 39,5m

Appendix 5: Location of images used in thesis

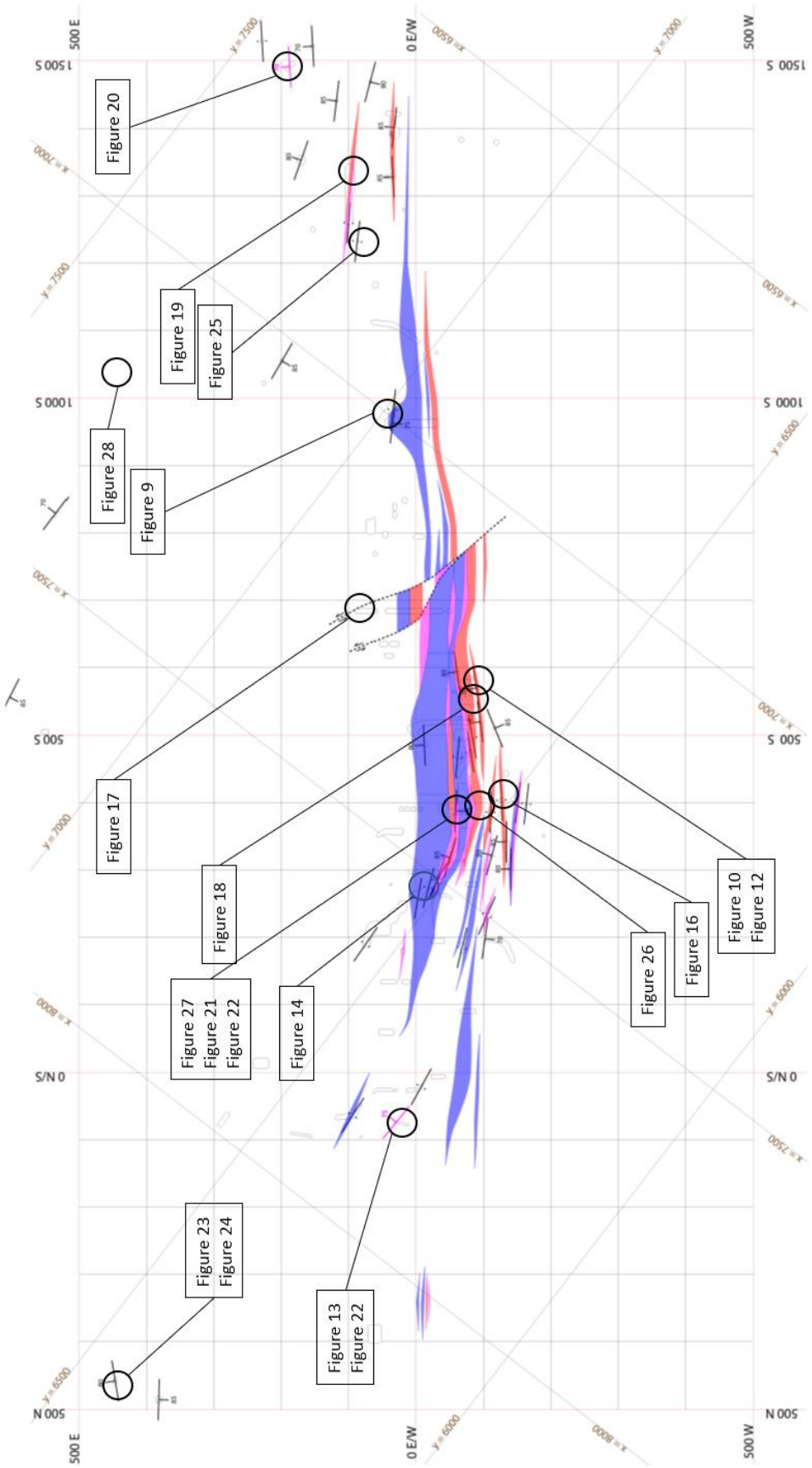

Figure 29 - Image locations